



OPEN ACCESS

EDITED BY

Alireza Nouri,
RMIT University, Australia

REVIEWED BY

Mediha Kök,
Firat University, Türkiye
Farzad Hamdi,
Martin Luther University of Halle-
Wittenberg, Germany

*CORRESPONDENCE

Kadri C. Atli,
✉ catli@tamu.edu

SPECIALTY SECTION

This article was submitted to Physical Properties of Metals, a section of the journal Frontiers in Metals and Alloys

RECEIVED 01 January 2023

ACCEPTED 08 March 2023

PUBLISHED 17 March 2023

CITATION

Atli KC and Karaman I (2023), A short review on the ultra-high temperature mechanical properties of refractory high entropy alloys.

Front. Met. Alloy 2:1135826.

doi: 10.3389/ftmal.2023.1135826

COPYRIGHT

© 2023 Atli and Karaman. This is an open-access article distributed under the terms of the [Creative Commons Attribution License \(CC BY\)](https://creativecommons.org/licenses/by/4.0/). The use, distribution or reproduction in other forums is permitted, provided the original author(s) and the copyright owner(s) are credited and that the original publication in this journal is cited, in accordance with accepted academic practice. No use, distribution or reproduction is permitted which does not comply with these terms.

A short review on the ultra-high temperature mechanical properties of refractory high entropy alloys

Kadri C. Atli* and I. Karaman

Department of Materials Science and Engineering, Texas A&M University, College Station, TX, United States

Mechanical properties of refractory high entropy alloys (RHEAs) at ultra-high temperatures (>1,100°C) are reviewed. Deformation behavior and strengthening mechanisms of select compositions are discussed. The limited number of studies portray remarkable mechanical properties of newly developed RHEA compositions at temperatures beyond the melting point of commercial Ni-based superalloys. Yet, the lack of quasi-static tensile deformation data and application relevant creep deformation data indicates RHEAs are still far from being reliable alternatives to Ni-based superalloys as high temperature structural materials. Future studies should concentrate on tensile deformation and creep of these new alloys systems at very high temperatures.

KEYWORDS

refractory materials, high entropy alloys, alloy design, mechanical properties, microstructural properties

1 Introduction

The development of superalloys, i.e., metallic materials with superior mechanical properties at elevated temperatures, began in the 1930s in the United States. This research was mainly driven by the need for more heat-resistant materials in aircraft engine turbosuperchargers. It has been paced in the 1940s by the increasing demands of the gas turbine engine technology, and in the early 1950s by space based nuclear reactor programs (Fawley et al., 1972; Philips et al., 2020). Ni-based superalloys with their unique combination of mechanical and physical properties at temperatures up to 1,150°C (Rame et al., 2020) have since been the staple structural material of high temperature applications. However, their use at higher operating temperatures is limited by their melting temperature.

The discovery of high entropy alloys (HEAs) has opened a new era in materials science leading to the development of fascinating alloy compositions with mechanical properties that conventional engineering alloys did not have, e.g., yield strengths greater than 1,000 MPa below 600°C or high strength and toughness at cryogenic temperatures (Miracle and Senkov, 2017; Senkov et al., 2018a). Unfortunately, these novel HEAs suffered the same high temperature problems as Ni-based superalloys, rendering them inefficient above 800°C. With the same founding motivation of HEAs, exploring the vast central regions of phase space bounded by refractory elements (Nb, Ta, Zr, Hf, Mo, and W) led to the development of refractory high entropy alloys (RHEAs) that could retain reasonable strength up to 1,600°C (Senkov et al., 2010; Senkov et al., 2018a). Poor high-temperature oxidation resistance and extreme oxygen sensitivity are some of the critical obstacles against the widespread implementation of refractory alloys, so elements beneficial for oxidation resistance (Al,

Cr, Ti, and Si) have been successfully doped to generate novel RHEA compositions with improved oxidation resistance (Gorr et al., 2017; Sheikh et al., 2018; Mueller et al., 2019). Another critical property for RHEAs is density that determines the extent of inertial stresses that can be generated inside the parts, which is especially a key concern for rotating machinery. Adding light metals such as Al, Ti or V has led to the development of several RHEA compositions with densities going as low as $5.45 \text{ g}\cdot\text{cm}^{-3}$ (Miracle and Senkov, 2017). Unsurprisingly, there is a compromise between lightweight and high temperature strength, i.e., most dense alloys are usually the ones that show the highest elevated temperature strength, e.g., MoNbTaW with a compressive yield strength of 400 MPa at $1,600^\circ\text{C}$.

Since their inception in early 2010s, there has been an exponentially increasing research effort on the development of RHEAs, with research areas focusing on alloy design using computational methods, analytical models, and selection rules; mechanical and microstructural characterization, oxidation properties, phase stability and strengthening mechanisms. As of December 2022, a quick search on the topic of “refractory high entropy alloys” in Web of Science returns a total of 1,360 publications, 790 of which were published since January 2020. In such a rapid progressing scientific field, it is very easy for researchers to get overwhelmed with the sheer amount published research each month and thus it is technically not feasible to publish an exhaustive review paper on all aspects of RHEAs to summarize the entire progress up to date.

This paper reviews the ultra-high temperature mechanical properties of RHEAs, which the authors deem as an important area for the implementation of these alloys in real world applications. “Ultra-high” temperature is defined to be above $1,100^\circ\text{C}$, the highest application temperature of state-of-the-art Ni-based superalloys (Rame et al., 2020), and the temperature above which technological difficulties associated with testing start to become more pronounced. For a more comprehensive review on RHEAs covering various other aspects such as strengthening mechanisms, alloy developments, phase stability and oxidation behavior, the reader can refer to (Miracle and Senkov, 2017; Senkov et al., 2018a; Senkov et al., 2019; George et al., 2020; Gorr et al., 2021). The goal of the present paper is to compare the ultra-high temperature mechanical properties of RHEAs with a discussion on their hot-deformation behavior, provide a background on the latest advancements in these RHEA systems, and discuss the potential future directions for ultra-high temperature RHEA research. As will be portrayed in the following sections, nearly all studies on the mechanical properties of RHEAs above $1,100^\circ\text{C}$ in open literature investigate the isothermal quasi-static deformation behavior under compression. There are also a few recent studies on the tensile creep deformation behavior of RHEAs, which will be reviewed in this paper.

2 Fabrication and processing of RHEAs

The lack of studies on the ultra-high temperature mechanical properties of RHEAs is partly due to the high costs and technical challenges associated with testing, the main contributor being the generation and maintenance of a highly protective atmosphere for

the oxygen sensitive test samples. Even at extremely low vacuum levels as low as 10^{-6} torr, oxidation of RHEAs is a typical problem with mechanical testing which affects the real mechanical behavior of the material at elevated temperatures. RHEAs are notorious for easily forming volatile or porous and fast-growing oxides in environments with the presence of oxygen. Since conventional high temperature steels dramatically soften or melt at ultra-high temperatures, grips or platens used for testing RHEAs are usually fabricated from high temperature ceramics, such as SiC, that can withstand temperatures up to $1,600^\circ\text{C}$ (Senkov et al., 2011). This brings additional difficulties in terms of testing since ceramics in general cannot sustain prolonged static or cyclic loads as good as metals.

Given the fact that metallic materials typically exhibit a dramatic decrease in their strengths above $0.6 T_m$, where T_m is the absolute melting temperature, including refractory elements with high T_m is a rational method to increase the overall T_m of the alloy and to render it a potential candidate for high temperature applications. All RHEA compositions in literature which are designed to operate at elevated temperatures include at least one element from the high melting point refractory elements Nb, Ta, Zr, Hf, Mo, and W. Other alloying elements are usually added to improve the oxidation resistance and lower the density of the alloy for light weighting. The alloys reviewed in this study are usually fabricated using two methods:

2.1 Ingot metallurgy

This process involves mixing and melting (e.g., arc-melting, levitation melting, plasma melting, e-beam melting, etc.) high-purity elements under a protective Argon atmosphere or in vacuum followed by solidification on a copper hearth or crucible. The process is followed by remelting the ingots several times for compositional homogenization. Additional annealing or homogenization steps are typically required to homogenize the microstructure as well as to establish a single-phase solid solution in RHEAs.

2.2 Powder metallurgy

Due to several alloying constituents in RHEAs, which typically have large differences in melting temperatures, ingot metallurgy methods may result in multiphase and/or dendritic structures with the problem of severe segregation even if the alloy undergoes heat treatments following the casting process. Powder metallurgy methods such as hot isostatic pressing (HIP), spark plasma sintering (SPS), or additive manufacturing employ the use of a mixture of elemental powders or prealloyed powders to precisely set the alloy composition. In the case of SPS, powder can be sintered in a very short time yielding a multicomponent alloy, however, unless the elemental powders are highly melted and the cooling rate is very rapid, the samples may feature incomplete mixing, which should not be an issue with the prealloyed powders (Senkov et al., 2018a; Philips et al., 2020).

TABLE 1 Composition, density, yield strength, specific yield strength, and plastic strain obtained before fracture under compression for RHEAs which have reported mechanical properties above 1,100°C. Tensile properties of commercially available high temperature materials Inconel 718, Haynes 230 and CMSX-4 are also included at the end of the table.

Alloy	Density (g·cm ⁻³)	Yield strength (MPa)	Specific yield strength (MPa·cm ³ ·g ⁻¹)	Plastic strain (mm/mm)	References
AlCrMoTi	5.98	100 at 1,200°C	16.72 at 1,200°C	—	Senkov et al. (2019)
AlCrMoNbTi	6.56	105 at 1,200°C	16.00 at 1,200°C	>0.24 at 1,200°C	Chen et al. (2016)
AlCr _{1.3} NiTi ₂	6.43	240 at 1,100°C	37.32 at 1,100°C	>0.50 at 1,100°C	Wang et al. (2021)
Al _{0.4} Hf _{0.6} NbTaTiZr	9.08	89 at 1,200°C	9.80 at 1,200°C	—	Senkov et al. (2019)
AlMoNbTi	6.64	200 at 1,200°C	30.12 at 1,200°C	—	Chen et al. (2018)
AlMo _{0.5} NbTa _{0.5} TiZr	7.14	250 at 1,200°C	35.01 at 1,200°C	>0.50 at 1,200°C	Senkov et al. (2016), Senkov et al. (2018b)
Al _{0.2} NbTaTiV	8.86	275 at 1,100°C	31.04 at 1,100°C	>0.30 at 1,100°C	Xiang et al. (2020)
		142 at 1,200°C	16.03 at 1,200°C	>0.30 at 1,200°C	
AlNbTi ₃ VZr _{1.5}	5.45	17 at 1,100°C	3.12 at 1,100°C	>0.70 at 1,100°C	Yu et al. (2022)
		13 at 1,150°C	2.38 at 1,150°C	>0.70 at 1,150°C	
		9 at 1,200°C	1.65 at 1,200°C	>0.70 at 1,200°C	
		7 at 1,250°C	1.28 at 1,250°C	>0.70 at 1,250°C	
CrMo _{0.5} NbTa _{0.5} TiZr	7.98	170 at 1,200°C	21.30 at 1,200°C	—	
CrNbTaTi	9.35	20 at 1,200°C	2.14 at 1,200°C	>0.69 at 1,200°C	Butler et al. (2021)
CrNbTiZr	6.56	32 at 1,200°C	4.88 at 1,200°C	—	Senkov et al. (2019)
HfMo _{0.5} NbSi _{0.7} TiV _{0.5}	8.49	235 at 1,200°C	27.68 at 1,200°C	>0.35 at 1,20°C	Liu et al. (2017)
HfMoNbTaTiZr	9.97	556 at 1,200°C	55.77 at 1,200°C	>0.30 at 1,200°C	Juan et al. (2015)
HfMoNbTaTiWZr	11.09	703 at 1,200°C	63.39 at 1,200°C	>0.35 at 1,200°C	Wang et al. (2019)
HfMoNb ₂ TaTi ₂ VWZr	9.72	292 at 1,200°C	30.04 at 1,200°C	>0.35 at 1,200°C	Yao et al. (2021)
Hf _{0.5} MoNbTaW	13.59	859 at 1,200°C	63.21 at 1,200°C	0.20 at 1,200°C	Tseng et al. (2022)
		735 at 1,400°C	54.08 at 1,400°C	0.14 at 1,400°C	
		537 at 1,600°C	39.51 at 1,600°C	0.18 at 1,600°C	
HfMoNbTaW	13.56	954 at 1,200°C	70.35 at 1,200°C	0.20 at 1,200°C	Tseng et al. (2022)
		840 at 1,400°C	61.95 at 1,400°C	0.10 at 1,400°C	
		571 at 1,600°C	42.11 at 1,600°C	0.20 at 1,600°C	
HfMo _{0.5} NbTiV _{0.5}	8.96	60 at 1,200°C	6.70 at 1,200°C	—	Senkov et al. (2019)
HfMoNbTiZr	8.70	397 at 1,100°C	45.63 at 1,100°C	>0.70 at 1,100°C	Guo et al. (2015), Guo et al. (2016), Dong et al. (2020)
		187 at 1,200°C	21.49 at 1,200°C	0.65 at 1,200°C	
HfMoScTaZr	9.28	498 at 1,200°C	53.66 at 1,200°C	>0.42 at 1,200°C	Nie et al. (2021)
HfMoTaTiZr	10.24	404 at 1,200°C	39.45 at 1,200°C	>0.30 at 1,200°C	Juan et al. (2015)
HfNbTaTiZr	9.94	92 at 1,200°C	9.26 at 1,200°C	>0.50 at 1,200°C	Senkov et al. (2012), Malek et al. (2019), Wang et al. (2019)
HfNbTaTiWZr	11.21	345 at 1,200°C	30.78 at 1,200°C	>0.35 at 1,200°C	Wang et al. (2019)
HfTa _{0.2} Ti ₂ V _{0.5} Zr	7.79	24 at 1,100°C	3.08 at 1,100°C	>0.70 at 1,100°C	Li et al. (2022)
MoNbSiTaTiV	8.00	718 at 1,200°C	89.75 at 1,200°C	0.43 at 1,200°C	Ge et al. (2022)
MoNbTaTiW	11.76	173 at 1,600°C	14.71 at 1,600°C	>0.25 at 1,600°C	Kalali et al. (2021), Wan et al. (2021), Wei et al. (2021)

(Continued on following page)

TABLE 1 (Continued) Composition, density, yield strength, specific yield strength, and plastic strain obtained before fracture under compression for RHEAs which have reported mechanical properties above 1,100°C. Tensile properties of commercially available high temperature materials Inconel 718, Haynes 230 and CMSX-4 are also included at the end of the table.

Alloy	Density (g·cm ⁻³)	Yield strength (MPa)	Specific yield strength (MPa·cm ³ ·g ⁻¹)	Plastic strain (mm/mm)	References
MoNbTaTiV	9.38	68 at 1,100°C	7.25 at 1,100°C	>0.35 at 1,100°C	Liu et al. (2021)
		45 at 1,200°C	4.80 at 1,200°C	>0.35 at 1,200°C	
		30 at 1,300°C	3.20 at 1,300°C	>0.35 at 1,300°C	
MoNbTa _{0.5} V	9.65	697 at 1,200°C	72.23 at 1,200°C	0.35 at 1,200°C	Zheng et al. (2022)
MoNbTaW	13.64	506 at 1,200°C	37.10 at 1,200°C	>0.25 at 1,200°C	Senkov et al. (2011)
		421 at 1,400 °C	30.86 at 1,400°C	>0.25 at 1,400°C	
		405 at 1,600°C	29.69 at 1,600°C	>0.25 at 1,600°C	
MoNbTaVW	12.35	735 at 1,200°C	59.51 at 1,200 °C	0.08 at 1,200 °C	Senkov et al. (2011)
		656 at 1,400 °C	53.12 at 1,400 °C	0.14 at 1,400 °C	
		477 at 1,600 °C	38.62 at 1,600°C	0.18 at 1,600°C	
(Mo ₂ C) _{0.2} NbTaW _{0.5}	12.99	1,026 at 1,200°C	78.98 at 1,200°C	>0.30 at 1,200°C	Wu et al. (2021)
		697 at 1,400°C	53.65 at 1,400°C	>0.40 at 1,400°C	
MoNbTiVZr	7.27	116 at 1,200°C	15.96 at 1,200°C	—	Senkov et al. (2019)
MoReTaW	16.75	172 at 1,600°C	10.27 at 1,600°C	>0.25 at 1,600°C	Wan et al. (2022)
NbRe _{0.3} TiZr	7.81	89 at 1,200°C	11.40 at 1,200°C	—	Senkov et al. (2019)
NbTaTiZr	8.92	60 at 1,100°C	6.73 at 1,100°C	>0.70 at 1,100°C	Wang et al. (2023)
		36 at 1,200°C	4.04 at 1,200°C	>0.70 at 1,200°C	
NbTaTiVZr	8.43	78 at 1,200°C	9.25 at 1,200°C	—	Senkov et al. (2019)
CMSX-4	8.70	420 at 1,094°C	48.28 at 1,094°C	0.40 at 1,094°C	Sengupta et al. (1994)
		146 at 1,204°C	16.78 at 1,204°C	0.39 at 1,204°C	
Inconel 718	8.22	105 at 1,200°C	12.77 at 1,200°C	0.70 at 1,200°C	Bhujangrao et al. (2020)
Haynes 230	8.97	76 at 1,095°C	8.47 at 1,095°C	0.83 at 1,095°C	Haynes International (2021)
		47 at 1,150°C	5.24 at 1,150°C	1.06 at 1,150°C	
		30 at 1,205°C	3.34 at 1,205°C	1.09 at 1,205°C	

3 Ultra-high temperature mechanical behavior of RHEAs

The ultra-high temperature behavior of RHEAs will be investigated in two sections. As mentioned earlier, there are only a few studies on the creep deformation behavior of RHEAs, while most of the studies are on the isothermal quasi-static deformation behavior.

3.1 Isothermal quasi-static deformation behavior

Table 1 lists RHEA compositions that have been quasi-statically deformed at temperatures higher than 1,100°C. Along with the compositions of the alloys, density, yield strength (YS), specific yield strength (SYS) and maximum plastic strain values (if available)

are also listed. All compositions were tested under compression with a strain rate of 0.001 s⁻¹. Figures 1, 2 are a summary of Table 1, portraying the variation of YS and SYS for selected RHEAs as a function of testing temperature, respectively. At a first glance to Table 1, one can see the density of different RHEA compositions ranging from 5.45 to as high as 16.75 g·cm⁻³. In this review, the RHEA compositions will be classified in three categories: as “low-density”, for alloys with densities smaller than 8 g·cm⁻³, as “medium-density” for alloys with density values ranging between 8 and 11 g·cm⁻³, and “high-density” for alloys which have densities larger than 11 g·cm⁻³.

3.1.1 Low-density RHEAs ($\rho < 8 \text{ g}\cdot\text{cm}^{-3}$)

Among the low-density RHEAs which have mechanical behavior data reported at ultra-high temperatures, the main constituent elements providing low density are Al, Cr, V, Ti, and Zr, along with the typical high-density refractory elements

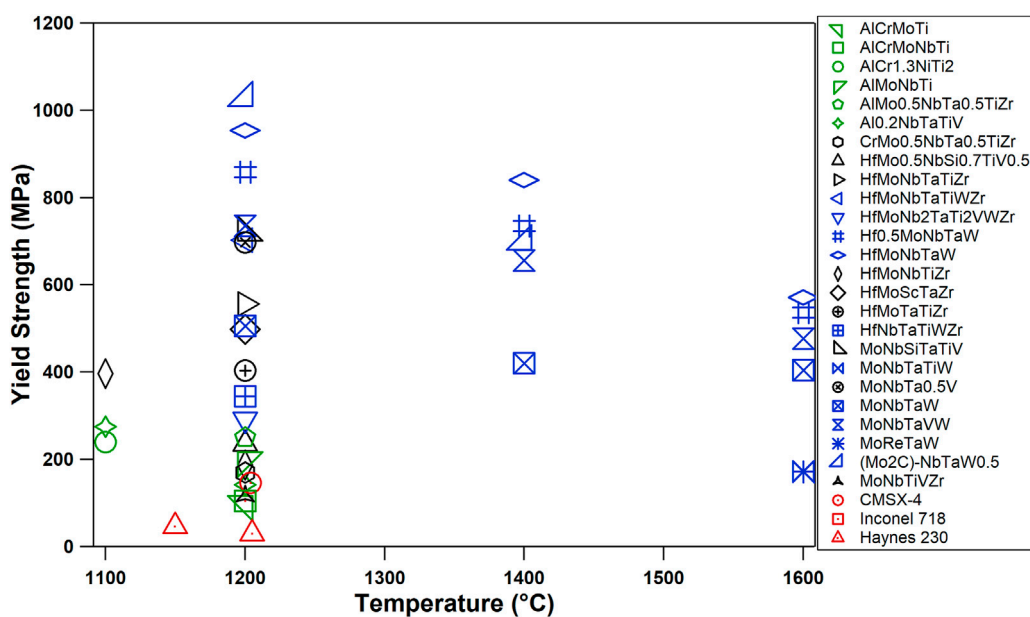


FIGURE 1 Temperature dependence of yield strength (YS) for RHEAs and commercial Ni-based superalloys (shown with red markers). Results are from quasi-static compression tests at a 0.001 s⁻¹ strain rate. Alloys containing Al and W are shown with green and blue markers, respectively.

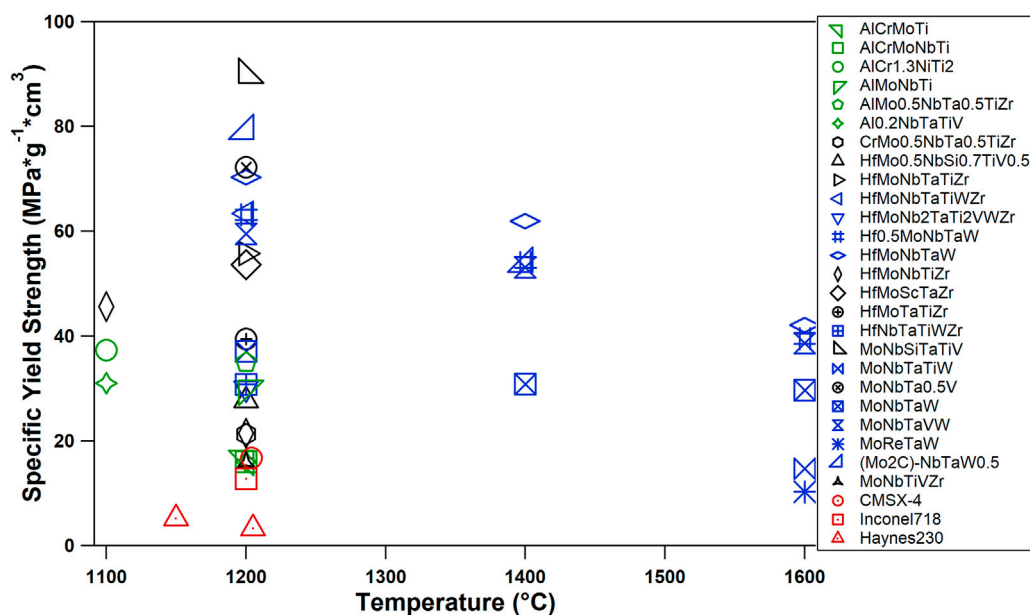


FIGURE 2 Temperature dependence of specific yield strength (SYS) for RHEAs and commercial Ni-based superalloys (shown with red markers). Results are from quasi-static compression tests at a 0.001 s⁻¹ strain rate. Alloys containing Al and W are shown with green and blue markers, respectively.

such as Mo, Nb, and Ta. It should be noted that a secondary motivation for the development of these RHEAs is to obtain enhanced oxidation properties through the formation of protective oxide films while maintaining adequate strength at relatively high operating temperatures (e.g., from room

temperature up to 1,000°C). As expected, these alloys do not exhibit as high strength values at ultra-high temperatures as medium-density and high-density RHEAs partly due to the lower melting points of constituent elements and as a result the lower T_m of the alloy.

Yield strength values of low-density RHEAs are notably low at ultra-high temperatures, typically below 100 MPa, going as low as 7 MPa at 1,200°C. There are two low-density compositions that stand out in Table 1 with exceptional mechanical properties, which are AlMo_{0.5}NbTa_{0.5}TiZr (Senkov et al., 2019), AlCr_{1.3}NiTi₂ (Wang et al., 2021) and the equiatomic AlCrMoNbTi (Chen et al., 2016). Although AlCr_{1.3}NiTi₂ (Wang et al., 2021) does not contain any refractory elements, thus cannot be classified as a RHEA, it is still included in Table 1 as it exhibits higher strength values than several reported low-density and medium-density RHEAs at 1,100°C as a high temperature high entropy alloy.

AlMo_{0.5}NbTa_{0.5}TiZr is one of the first RHEAs that has been shown to exhibit superior high temperature strength compared to Ni-based superalloys (Senkov et al., 2018b). The high performance of this alloy is attributed to the presence of BCC coherent nanoprecipitates in an ordered B2 matrix, along with coarse HCP particles at grain boundaries. The nanoscale two-phase structure displays good thermal stability, with a YS of 250 MPa at 1,200°C and a corresponding SYS of 35 MPa·cm³·g⁻¹.

AlCr_{1.3}NiTi₂ is a eutectic RHEA composed of BCC and Heusler-like L₂₁ phases exhibiting an ultrafine lamellar structure, with interlamellar spacing about 400 nm. The alloy has a YS of 240 MPa and a SYS of 37.3 MPa·cm³·g⁻¹ at 1,100°C. By comparison, conventional high temperature alloy Haynes 230 has a YS of 76 MPa and a SYS of 8.5 MPa·cm³·g⁻¹ at 1,095°C, while Inconel 718 has a YS of 130 MPa and SYS of 15.82 MPa·cm³·g⁻¹ at 1,000°C. The alloy has outstanding softening resistance at temperatures as high as 1,100°C, which is attributed to the following features: 1) The presence of a near-equilibrium eutectic structure acting as an *in-situ* composite which can resist changes in temperatures as high as the eutectic reaction point, 2) presence of the Ni-Al-Ti rich L₂₁ phase with a high degree of order, limited slip systems and excellent creep resistance, 3) the semi-coherent eutectic phase interface with a high interfacial bonding strength, 4) high density of coherent nanoprecipitates within the L₂₁ phase increasing the overall strength of the RHEA *via* precipitation strengthening (Wang et al., 2021).

Single phase AlCrMoNbTi RHEA exhibits a YS of 105 MPa during compression testing at 1,200°C. This RHEA exhibits an increased level of plasticity with no thermal softening, and a ductility of at least 24% at this temperature. Electron backscatter diffraction analyses of the samples deformed at 1,200°C revealed the formation of hexagonal Laves phase and another unknown phase rich in Cr within the grains (Chen et al., 2016). This indicates that there might be issues with the phase stability of some low-density RHEA compositions at ultra-high temperatures and more detailed phase stability analyses should be performed.

3.1.2 Medium-density RHEAs ($8 \leq \rho < 11 \text{ g}\cdot\text{cm}^{-3}$)

For medium-density RHEAs, it is observed from Table 1 that low-density elements with relatively high melting points such as Ti, V or Zr are usually preferred instead of Al. When YS and SYS values are compared, three medium-density RHEA compositions show superior performance compared to others, i.e., the equiatomic MoNbSiTaTiV, MoNbTa_{0.5}V, and equiatomic HfMoScTaZr.

Equiatomic MoNbSiTaTiV is a hypoeutectic composite RHEA, composed of a BCC phase and *in-situ* precipitated Ti₅Si₃ silicide

phase (Ge et al., 2022). The RHEA exhibits a YS of 718 MPa at 1,200°C despite the lack of a high concentration of high T_m refractory elements. The alloy has a relatively low density of 8 g·cm³ due to the addition of a large atomic percentage of Si. This results in a SYS of 89.75 MPa·cm³·g⁻¹, the highest SYS value recorded at 1,200°C and above for a RHEA to the best of the author's knowledge. Interestingly, this RHEA exhibits brittle fracture at 1,000°C and below due to the presence of the brittle Ti₅Si₃ phase and low-plasticity BCC matrix. However, deformation at 1,200°C takes place with the formation of refined crystal grains due to dynamic recrystallization, greatly enhancing the compressive plastic strain of the material up to 43%. At 1,200°C, the high strength of the RHEA is attributed to solid solution strengthening effect of Si in the matrix, the strengthening effect of the Ti₅Si₃ silicide phase, and the interface strengthening effect of the lamellar eutectic structure (Ge et al., 2022).

Achieving both RT and elevated temperature strength and ductility is one of the key challenges in RHEA research. Unlike the equiatomic multi-phase MoNbSiTaTiV, the as-cast single phase MoNbTa_{0.5}V with a dendritic structure shows improved strength and ductility at both ambient and ultra-high temperatures (Zheng et al., 2022). This RHEA also has remarkable mechanical properties at 1,200°C, i.e., a YS of 697 MPa, a SYS of 72.23 MPa·cm³·g⁻¹ and a ductility of 35%. The improved high temperature performance of this RHEA is attributed to the thermal stability of grain boundaries and the retarded recrystallization process. This results in the retention of high strength levels and induces a milder softening response at ultra-high temperatures compared to other medium-density RHEAs.

Scandium (Sc) is a rare Earth metal with the advantages of high T_m, low density and good ductility. Sc has been successfully used as an alloying element in RHEA compositions, giving the alloy high temperature strength, structural stability, weldability and corrosion resistance (Rogal et al., 2016; Takeuchi et al., 2016). Equiatomic HfMoScTaZr RHEA exhibits a single BCC phase from ambient temperature up to 1,300°C (Nie et al., 2021). This alloy has a relatively low density of 9.28 g·cm³ owing to the light constituent elements Sc and Zr. YS at 1,200°C is reported as 498 MPa, with the alloy exhibiting a softening behavior, dropping in strength to around 200 MPa at a strain level of 42% without failure. Compared to conventional high temperature alloys such as Inconel 718 or CMSX-4, diffusion-controlled processes take place in HfMoScTaZr RHEA at a much higher temperature due to the overall higher T_m of the alloy.

3.1.3 High-density RHEAs ($\rho \geq 11 \text{ g}\cdot\text{cm}^{-3}$)

RHEAs with density values above 11 g·cm³ typically include the heavy refractory elements such as W, Ta, and Hf. These alloys usually have the highest T_m among all other RHEAs, and thus can retain their strength at temperatures above 1,400°C. Some of these RHEA compositions exhibit remarkable strength values, e.g., MoNbTaW and MoNbTaVW as shown in the pioneering study of Senkov et al. (2011), but they do not possess SYS values as high as the medium-density RHEAs due to their relatively high densities. While these RHEAs are not ideal to be candidates for lightweight applications (e.g., aerospace, automotive), they are most likely to find their places in ultra-high temperature applications where

inertial effects are not a design constraint (e.g., nuclear reactors and fusion reactors).

Equiatomic HfMoNbTaW features a single BCC phase after a homogenization heat treatment at 2,100°C for 2 h (Tseng et al., 2022). This RHEA has a YS of 571 MPa at 1,600°C, which is higher than the early heavy RHEA compositions MoNbTaW or MoNbTaVW, that were discovered more than a decade ago. The alloy exhibits a constant YS of approximately 950 MPa between 800 and 1,200°C, above which diffusion-controlled processes start to control the deformation behavior. The improved mechanical properties of this RHEA over MoNbTaW or MoNbTaVW is mainly attributed to the solid-solution hardening effect by Hf addition. Hf, as an alloying element, proved to be the optimal choice with its high melting point, low shear modulus and high atomic radius, that yielded the greatest solid solution strengthening contribution among other elements per equation:

$$\Delta\sigma_i = AGf_i^{4/3}c_i^{2/3}$$

where $\Delta\sigma_i$ is the solid solution strengthening caused by the i th element in the alloy, A is a dimensionless material constant of the order of 0.04, G is the shear modulus of the alloy, c_i is the atomic fraction of element i , and f_i is the mismatch parameter of element i , which is related to its shear modulus and atomic size (Yao et al., 2017).

Another high-density RHEA composition that deserves a special mention is $(\text{Mo}_2\text{C})_{0.2}\text{NbTaW}_{0.5}$. This composition is based on the ternary NbTaW_{0.5} refractory alloy. The resulting composite with the addition of Mo₂C consists of a disordered BCC solid-solution phase and HCP Mo₂C carbide phase. Similar to silicide strengthening shown in the medium-density MoNbSiTaTiV, this RHEA is another example for the recent scientific focus that has shifted from designing single phase BCC RHEA solid solutions to multi-phase composite structures strengthened by precipitation, dispersions, and interfaces. $(\text{Mo}_2\text{C})_{0.2}\text{NbTaW}_{0.5}$ alloy could maintain an extremely high strength of 697 MPa at 1,400°C resulting in a SYS of 53.65 MPa·cm³·g⁻¹ (Wu et al., 2021). Mo₂C carbides played a crucial role in the retention of strength at high temperatures, by impeding dislocation movement. They also precipitated along the grain boundaries preventing or impeding their sliding and rotation, which in turn greatly increased the YS at ultra-high temperatures (Wu et al., 2021).

HfNbTaTiZr is a medium-density single BCC phase RHEA with mediocre ultra-high temperature mechanical properties. The RHEA has a YS of 92 MPa at 1,200°C (Senkov et al., 2012; Malek et al., 2019; Wang et al., 2019). Recent attempts to improve the high-temperature performance of this alloy involved the use of W and Mo alloying additions (Wang et al., 2019). Evidently, these refractory elements had the highest T_m among the four refractory elements that were not originally included in the RHEA (i.e., W, Mo, Cr, and V) and they were intended to increase the overall T_m , thereby elevating the softening temperatures. HfMoNbTaTiWZr has a YS of 703 MPa at 1,200°C, and a SYS of 63.39 MPa·cm³·g⁻¹. Unlike HfNbTaTiZr, this RHEA has a dual BCC structure, which has a strong influence on the improved high temperature mechanical properties. It is hypothesized that increased density of phase boundaries act as obstacles against dislocation motion. In

addition, both W and Mo elements have solid solution strengthening effects (Wang et al., 2019).

3.2 Creep behavior

Tensile creep resistance is one of the key properties of a material to be used in high temperature structural applications. Despite the availability of a large amount of high temperature quasi-static compression behavior data for RHEAs dating back to 2010, there is a lack of tensile creep data. This is not a coincidence, as there are only a few isothermal quasi-static tensile test results for RHEAs, which have been recorded at high temperature.

The tensile creep properties of HfNbTaTiZr RHEA have recently been reported and compared to the properties of a commercially available single crystal of CMSX-4 alloy at 1,100°C (Gadelmeier et al., 2022). The RHEA is dramatically weaker in creep than both the precipitation hardened CMSX-4 single crystal alloy and the solid solution matrix of CMSX-4 excluding the effects of precipitation hardening. The RHEA also undergoes stress-assisted phase decomposition during creep testing. While the YS values of two alloys are similar as seen in Table 1 (92 and 146 MPa at 1,200°C for the RHEA and CMSX-4, respectively), it should be noted that the values for CMSX-4 are in tension and CMSX-4 has a much lower T_m of 1,330°C, compared to 1,937°C for HfNbTaTiZr RHEA. One possible reason for this intriguing underperformance of the RHEA in tensile creep, despite similar mechanical properties and increased T_m is that the tested RHEA had a more open BCC structure than the close-packed FCC structure of CMSX-4, allowing a faster diffusion of the constituent elements.

A more recent study reported the tensile creep properties of HfNbTaTiZr RHEA up to 1,250°C under stress levels of 5–30 MPa (Liu et al., 2022). The creep behavior was related to the solute drag mechanism evidenced by the stress exponent n ranging between 2.5 and 2.8. The creep activation energies were found as 273 ± 15 kJ·mol⁻¹ and according to diffusivity calculation and solute drag creep model prediction, the creep rate was found to be controlled by the diffusivity of Ta, that impeded the dislocation motion during creep deformation.

4 Concluding remarks

The vast compositional space available for RHEA design fueled worldwide research efforts on computational materials development since 2010, searching for the ultimate RHEA compositions, especially for high temperature strength. Several compositions with remarkable physical and mechanical properties have been developed that are potential alternatives to conventional Ni-based superalloys. On the experimental side, the fact that there is not a single study reporting the high temperature quasi-static tensile properties of RHEAs points out two critical problems. Ultra-high temperature tensile testing is technologically challenging and expensive. The key materials-related difficulty with tensile testing is the inherent brittle behavior and poor machinability of the load bearing parts of the testing device. These parts must be strong and tough enough at both ambient and elevated temperatures to test RHEAs with the highest melting temperatures. SiC platens have successfully been utilized for compression testing at temperatures as high as 1,600°C (Senkov et al., 2011), but the use of SiC grips for ultra-high temperature testing of RHEAs is not possible due to the brittleness of SiC. There are commercial

tensile testing systems with tensile grips made of pure tungsten or the Molybdenum alloy TZM, however, at high temperatures, their yield strengths are lower than some of the potential RHEAs, which require special grip designs. Secondly, unlike traditional alloys with one or two base elements, RHEAs with multiple principal elements have poor processability. While this review paper only reports the mechanical properties of RHEAs at ultra-high temperatures, the reader should not get the misconception that these RHEAs display same or better mechanical properties at ambient temperatures. It has always been a grand challenge to develop RHEAs with improved mechanical properties at both ambient and elevated temperatures. BCC RHEAs are inherently more brittle compared to FCC alloys due to increased lattice friction against dislocation motion. In addition, refractory elements such as Mo, Zr, and W have relatively high ductile-to-brittle transition temperatures that contribute to the brittleness of RHEAs at ambient temperatures. Therefore, it is difficult to machine tension specimens out of brittle ingots of RHEAs, and even if a specimen is successfully prepared, any defects present in the form of microcracks, inclusions or porosities (exacerbated with oxidation at high temperatures, and the evaporation of those oxides) that were introduced during fabrication or processing may lead to early catastrophic failure during tensile loading because of the low fracture toughness of the specimens.

Despite the encouraging ultra-high temperature strength values of RHEAs reviewed in this study, more relevant data for structural applications is needed to better assess the potential of these RHEAs. The results of compression tests performed at relatively higher strain rates (e.g., 0.001 s^{-1}) cannot be used to reliably deduce the behavior of the material under constant load at much lower strain rates, i.e., under creep conditions. This has recently been demonstrated in HfNbTaTiZr (Gadelmeier et al., 2022), as the tensile creep performance of the RHEA was found to be inferior to that of CMSX-4, although the alloys had similar mechanical properties at elevated temperatures and HfNbTaTiZr had a greater T_m . Therefore, it is of paramount importance that creep-relevant properties of the newly developed RHEAs should be measured before these alloys can be proposed as alternatives to Ni-based superalloys. Oxidation will always remain as a major obstacle against the implementation of these refractory element based alloys in high temperature applications. Density is another critical parameter that must be considered when designing for lightweighting and reducing inertial stresses in rotating parts. Both the density and oxidation resistance of novel RHEAs must be improved by alloy design without deteriorating the mechanical properties.

There is a vast body of knowledge on all aspects of conventional Ni-based superalloys after decades of research. This knowledge is necessary for the successful

commercialization of a newly developed alloy system, which might take years or even decades depending on the application area. In this respect, as the research on RHEA progresses at full throttle in multiple areas ranging from mechanical properties, phase stability, strengthening mechanisms, deformation behavior at a wide range of temperatures to a deep understanding of oxidation/corrosion behavior, microstructural and thermophysical properties, the limited amount of data reviewed in this study for the mechanical properties of RHEAs at ultra-high temperature clearly portrays that RHEA research is still in its infancy after 12 years of its inception and there is still a long way to go for the full implementation of these RHEAs in high temperature structural applications.

Author contributions

KA: Data curation, writing—original draft, writing—review and editing. IK: Funding acquisition, writing—review and editing.

Funding

The authors acknowledge the support from the U.S. Department of Energy (DOE) ARPA-E ULTIMATE Program through Project DE-AR0001427 and NASA-ESI Program under Grant Number 80NSSC21K0223.

Conflict of interest

The authors declare that the research was conducted in the absence of any commercial or financial relationships that could be construed as a potential conflict of interest.

Publisher's note

All claims expressed in this article are solely those of the authors and do not necessarily represent those of their affiliated organizations, or those of the publisher, the editors and the reviewers. Any product that may be evaluated in this article, or claim that may be made by its manufacturer, is not guaranteed or endorsed by the publisher.

References

- Bhujangrao, T., Veiga, F., Suárez, A., Iriondo, E., and Mata, F. G. (2020). High-temperature mechanical properties of IN718 alloy: Comparison of additive manufactured and wrought samples. *Crystals* 10, 689. doi:10.3390/cryst10080689
- Butler, T. M., Senkov, O. N., Velez, M. A., and Daboiku, T. I. (2021). Microstructures and mechanical properties of CrNb, CrNbTi, and CrNbTaTi concentrated refractory alloys. *Intermetallics* 138, 107323. doi:10.1016/j.intermet.2021.107323
- Chen, H., Kauffmann, A., Gorr, B., Schliephake, D., Seemuller, C., Wagner, J. N., et al. (2016). Microstructure and mechanical properties at elevated temperatures of a new Al-containing refractory high-entropy alloy Nb-Mo-Cr-Ti-Al. *J. Alloys Compd.* 661, 206–215. doi:10.1016/j.jallcom.2015.11.050
- Chen, H., Kauffmann, A., Laube, S., Choi, I. C., Schwaiger, R., Huang, Y., et al. (2018). Contribution of lattice distortion to solid solution strengthening in a series of refractory high entropy alloys. *Metall. Mater. Trans. a-Phys. Metall. Mater. Sci.* 49A (3), 772–781. doi:10.1007/s11661-017-4386-1
- Dong, F. Y., Yuan, Y., Li, W. D., Zhang, Y., Liaw, P. K., Yuan, X. G., et al. (2020). Hot deformation behavior and processing maps of an equiatomic MoNbHfZrTi refractory high entropy alloy. *Intermetallics* 126, 106921. doi:10.1016/j.intermet.2020.106921
- Fawley, R. W. (1972). "Superalloy progress," in *The superalloys*. Editors C. T. Sims and W. C. Hagel
- Gadelmeier, C., Yang, Y., Glatzel, U., and George, E. P. (2022). Creep strength of refractory high-entropy alloy TiZrHfNbTa and comparison with Ni-base superalloy CMSX-4. *Cell Rep. Phys. Sci.* 3 (8), 100991. doi:10.1016/j.xcrp.2022.100991

- Ge, S. F., Lin, S. F., Fu, H. M., Zhang, L., Geng, T. Q., Zhu, Z. W., et al. (2022). High-temperature mechanical properties and dynamic recrystallization mechanism of *in situ* silicide-reinforced MoNbTaTiVSi refractory high-entropy alloy composite. *Acta Metall. Sin. English Lett.* 35, 1617–1630. doi:10.1007/s40195-022-01394-7
- George, E. P., Curtin, W. A., and Tasan, C. C. (2020). High entropy alloys: A focused review of mechanical properties and deformation mechanisms. *Acta Mater.* 188, 435–474. doi:10.1016/j.actamat.2019.12.015
- Gorr, B., Müller, F., Azim, M., Christ, H.-J., Müller, T., Chen, H., et al. (2017). High-temperature oxidation behavior of refractory high-entropy alloys: Effect of alloy composition. *Oxid. Metals* 88 (3), 339–349. doi:10.1007/s11085-016-9696-y
- Gorr, B., Schellert, S., Muller, F., Christ, H. J., Kauffmann, A., and Heilmaier, M. (2021). Current status of research on the oxidation behavior of refractory high entropy alloys. *Adv. Eng. Mater.* 23 (5), 2001047. doi:10.1002/adem.202001047
- Guo, N. N., Wang, L., Luo, L. S., Li, X. Z., Su, Y. Q., Guo, J. J., et al. (2015). Microstructure and mechanical properties of refractory MoNbHfZrTi high-entropy alloy. *Mater. Des.* 81, 87–94. doi:10.1016/j.matdes.2015.05.019
- Guo, N. N., Wang, L., Luo, L. S., Li, X. Z., Chen, R. R., Su, Y. Q., et al. (2016). Hot deformation characteristics and dynamic recrystallization of the MoNbHfZrTi refractory high-entropy alloy. *Mater. Sci. Eng. A-Struct. Mater. Prop. Microstruct. Process.* 651, 698–707. doi:10.1016/j.msea.2015.10.113
- Haynes International (2021). HAYNES® 230® alloy for cyclone separators tech brief for long-term performance in cyclone separators. Available from: [https://www.haynesintl.com/tech-briefs/high-temperature-alloys/high-temperature-alloy-applications/haynes-230-alloy-for-cyclone-separators-tech-brief-\(H-3060\)](https://www.haynesintl.com/tech-briefs/high-temperature-alloys/high-temperature-alloy-applications/haynes-230-alloy-for-cyclone-separators-tech-brief-(H-3060)).
- Juan, C. C., Tsai, M. H., Tsai, C. W., Lin, C. M., Wang, W. R., Yang, C. C., et al. (2015). Enhanced mechanical properties of HfMoTaTiZr and HfMoNbTaTiZr refractory high-entropy alloys. *Intermetallics* 62, 76–83. doi:10.1016/j.intermet.2015.03.013
- Kalali, D. G., Antharam, S., Hasan, M., Karthik, P. S., Phani, P. S., Rao, K. B. S., et al. (2021). On the origins of ultra-high hardness and strain gradient plasticity in multi-phase nanocrystalline MoNbTaTiW based refractory high-entropy alloy. *Mater. Sci. Eng. A-Struct. Mater. Prop. Microstruct. Process.* 812, 141098. doi:10.1016/j.msea.2021.141098
- Li, T. X., Lu, Y. P., Li, Z. Q., Wang, T. M., and Li, T. J. (2022). Hot deformation behavior and microstructure evolution of non-equimolar Ti2ZrHfV0.5Ta0.2 refractory high-entropy alloy. *Intermetallics* 146, 107586. doi:10.1016/j.intermet.2022.107586
- Liu, Y., Zhang, Y., Zhang, H., Wang, N. J., Chen, X., Zhang, H. W., et al. (2017). Microstructure and mechanical properties of refractory HfMo0.5NbTiV0.5Six high-entropy composites. *J. Alloys Compd.* 694, 869–876. doi:10.1016/j.jallcom.2016.10.014
- Liu, Q., Wang, G. F., Liu, Y. K., Sui, X. C., Chen, Y. Q., and Luo, S. Y. (2021). Hot deformation behaviors of an ultrafine-grained MoNbTaTiV refractory high-entropy alloy fabricated by powder metallurgy. *Mater. Sci. Eng. A-Struct. Mater. Prop. Microstruct. Process.* 809, 140922. doi:10.1016/j.msea.2021.140922
- Liu, C.-J., Gadelmeier, C., Lu, S.-L., Yeh, J.-W., Yen, H.-W., Gorsse, S., et al. (2022). Tensile creep behavior of HfNbTaTiZr refractory high entropy alloy at elevated temperatures. *Acta Mater.* 237, 118188. doi:10.1016/j.actamat.2022.118188
- Malek, J., Zyka, J., Lukac, F., Cizek, J., Kuncicka, L., and Kocich, R. (2019). Microstructure and mechanical properties of sintered and heat-treated HfNbTaTiZr high entropy alloy. *Metals* 9 (12), 1324. doi:10.3390/met9121324
- Miracle, D. B., and Senkov, O. N. (2017). A critical review of high entropy alloys and related concepts. *Acta Mater.* 122, 448–511. doi:10.1016/j.actamat.2016.08.081
- Mueller, F., Gorr, B., Christ, H.-J., Mueller, J., Butz, B., Chen, H., et al. (2019). On the oxidation mechanism of refractory high entropy alloys. *Corros. Sci.* 159, 108161. doi:10.1016/j.corsci.2019.108161
- Nie, X. W., Cai, M. D., and Cai, S. (2021). Microstructure and mechanical properties of a novel refractory high entropy alloy HfMoScTaZr. *Int. J. Refract. Metals Hard Mater.* 98, 105568. doi:10.1016/j.ijrmhm.2021.105568
- Philips, N. R., Carl, M., and Cunningham, N. J. (2020). New opportunities in refractory alloys. *Metall. Mater. Trans. A-Phys. Metall. Mater. Sci.* 51A, 3299–3310. doi:10.1007/s11661-020-05803-3
- Rame, J., Utada, S., Bortolucci Ormastroni, L. M., Mataveli-Suave, L., Menou, E., Després, L., et al. (2020). “Platinum-containing new generation nickel-based superalloy for single crystalline applications,” in *Superalloys 2020* (Springer), 71–81.
- Rogal, Ł., Czerwinski, F., Jochym, P. T., and Litynska-Dobrzynska, L. (2016). Microstructure and mechanical properties of the novel Hf25Sc25Ti25Zr25 equiatomic alloy with hexagonal solid solutions. *Mater. Des.* 92, 8–17. doi:10.1016/j.matdes.2015.11.104
- Sengupta, A., Putatunda, S. K., Bartosiewicz, L., Hangas, J., Nailos, P. J., Peputapeck, M., et al. (1994). Tensile behavior of a new single-crystal nickel-based superalloy (CMSX-4) at room and elevated temperatures. *J. Mater. Eng. Perform.* 3 (1), 73–81. doi:10.1007/bf02654502
- Senkov, O. N., Wilks, G. B., Miracle, D. B., Chuang, C. P., and Liaw, P. K. (2010). Refractory high-entropy alloys. *Intermetallics* 18 (9), 1758–1765. doi:10.1016/j.intermet.2010.05.014
- Senkov, O. N., Wilks, G. B., Scott, J. M., and Miracle, D. B. (2011). Mechanical properties of Nb25Mo25Ta25W25 and V20Nb20Mo20Ta20W20 refractory high entropy alloys. *Intermetallics* 19 (5), 698–706. doi:10.1016/j.intermet.2011.01.004
- Senkov, O. N., Scott, J. M., Senkova, S. V., Meisenkothen, F., Miracle, D. B., and Woodward, C. F. (2012). Microstructure and elevated temperature properties of a refractory TaNbHfZrTi alloy. *J. Mater. Sci.* 47 (9), 4062–4074. doi:10.1007/s10853-012-6260-2
- Senkov, O. N., Isheim, D., Seidman, D. N., and Pilchak, A. L. (2016). Development of a refractory high entropy superalloy. *Entropy* 18 (3), 102. doi:10.3390/e18030102
- Senkov, O. N., Miracle, D. B., Chaput, K. J., and Couzinie, J.-P. (2018a). Development and exploration of refractory high entropy alloys—a review. *J. Mater. Res.* 33 (19), 3092–3128. doi:10.1557/jmr.2018.153
- Senkov, O. N., Jensen, J. K., Pilchak, A. L., Miracle, D. B., and Fraser, H. L. (2018b). Compositional variation effects on the microstructure and properties of a refractory high-entropy superalloy AlMo0.5NbTa0.5TiZr. *Mater. Des.* 139, 498–511. doi:10.1016/j.matdes.2017.11.033
- Senkov, O. N., Gorsse, S., and Miracle, D. B. (2019). High temperature strength of refractory complex concentrated alloys. *Acta Mater.* 175, 394–405. doi:10.1016/j.actamat.2019.06.032
- Sheikh, S., Gan, L., Tsao, T. K., Murakami, H., Shafeie, S., and Guo, S. (2018). Aluminizing for enhanced oxidation resistance of ductile refractory high-entropy alloys. *Intermetallics* 103, 40–51. doi:10.1016/j.intermet.2018.10.004
- Takeuchi, A., Amiya, K., Wada, T., and Yubuta, K. (2016). Dual HCP structures formed in senary ScYLaTiZrHf multi-principal-element alloy. *Intermetallics* 69, 103–109. doi:10.1016/j.intermet.2015.10.022
- Tseng, K.-K., Huang, H.-H., Wang, W.-R., Yeh, J.-W., and Tsai, C.-W. (2022). Edge-dislocation-induced ultrahigh elevated-temperature strength of HfMoNbTaW refractory high-entropy alloys. *Sci. Technol. Adv. Mater.* 23 (1), 642–654. doi:10.1080/14686996.2022.2129444
- Wan, Y. X., Mo, J. Y., Wang, X., Zhang, Z. B., Shen, B. L., and Liang, X. B. (2021). Mechanical properties and phase stability of WTaMoNbTi refractory high-entropy alloy at elevated temperatures. *Acta Metall. Sin. English Lett.* 34, 1585–1590. doi:10.1007/s40195-021-01263-9
- Wan, Y. X., Wang, Q. Q., Mo, J. Y., Zhang, Z. B., Wang, X., Liang, X. B., et al. (2022). WReTaMo refractory high-entropy alloy with high strength at 1600 °C. *Adv. Eng. Mater.* 24 (2), 2100765. doi:10.1002/adem.202100765
- Wang, M., Ma, Z., Xu, Z., and Cheng, X. (2019). Microstructures and mechanical properties of HfNbTaTiZrW and HfNbTaTiZrMoW refractory high-entropy alloys. *J. Alloys Compd.* 803, 778–785. doi:10.1016/j.jallcom.2019.06.138
- Wang, M. L., Lu, Y. P., Wang, T. M., Zhang, C. A., Cao, Z. Q., Li, T. J., et al. (2021). A novel bulk eutectic high-entropy alloy with outstanding as-cast specific yield strengths at elevated temperatures. *Scr. Mater.* 204, 114132. doi:10.1016/j.scriptamat.2021.114132
- Wang, B., Shan, X., Zhao, H., Bai, S., Wang, B., Tian, Y., et al. (2023). High-temperature deformation behavior and microstructural evolution of NbZrTiTa refractory high entropy alloy. *J. Alloys Compd.* 936, 168059. doi:10.1016/j.jallcom.2022.168059
- Wei, W. C., Wang, T., Wang, C. Y., Wu, M., Nie, Y. P., and Peng, J. (2021). Ductile W0.4MoNbxCrTaTi refractory high-entropy alloys with excellent elevated temperature strength. *Mater. Lett.* 295, 129753. doi:10.1016/j.matlet.2021.129753
- Wu, S. Y., Qiao, D. X., Zhao, H. L., Wang, J., and Lu, Y. P. (2021). A novel NbTaW0.5(Mo2C)(x) refractory high-entropy alloy with excellent mechanical properties. *J. Alloys Compd.* 889, 161800. doi:10.1016/j.jallcom.2021.161800
- Xiang, L., Guo, W. M., Liu, B., Fu, A., Li, J. B., Fang, Q. H., et al. (2020). Microstructure and mechanical properties of TaNbVTiAlx refractory high-entropy alloys. *Entropy* 22 (3), 282. doi:10.3390/e22030282
- Yao, H. W., Qiao, J. W., Hawk, J. A., Zhou, H. F., Chen, M. W., and Gao, M. C. (2017). Mechanical properties of refractory high-entropy alloys: Experiments and modeling. *J. Alloys Compd.* 696, 1139–1150. doi:10.1016/j.jallcom.2016.11.188
- Yao, H. W., Miao, J. W., Liu, Y. M., Guo, E. Y., Huang, H., Lu, Y. P., et al. (2021). Effect of Ti and Nb contents on microstructure and mechanical properties of HfZrVTaMoWTi_xNb_y refractory high-entropy alloys. *Adv. Eng. Mater.* 23 (8), 2100225. doi:10.1002/adem.202100225
- Yu, Z., Xie, B., Zhu, Z., Xu, B., and Sun, M. (2022). High-temperature deformation behavior and processing maps of a novel AlNbTi3VZr1.5 refractory high entropy alloy. *J. Alloys Compd.* 912, 165220. doi:10.1016/j.jallcom.2022.165220
- Zheng, W., Lu, S., Wu, S., Chen, X., and Guo, W. (2022). Development of MoNbVTx refractory high entropy alloy with high strength at elevated temperature. *Mater. Sci. Eng. A-Struct. Mater. Prop. Microstruct. Process.* 850, 143554. doi:10.1016/j.msea.2022.143554